ELASE: Enabling Real-time Elastic Sensing Resource Scheduling in 5G vRAN

Yulong Chen[1,2], Junchen Guo[2], Yimiao Sun[1], Haipeng Yao[3], Yunhao Liu[1], Yuan He[1†]
[1]Tsinghua University, China [2]Alibaba Group, China [3]Beijing University of Posts and Telecommunications, China
yl-chen22@mails.tsinghua.edu.cn, junchen.gjc@alibaba-inc.com, sym21@mails.tsinghua.edu.cn,
yaohaipeng@bupt.edu.cn, yunhao@tsinghua.edu.cn, heyuan@tsinghua.edu.cn

2024 IEEE/ACM 32nd International Symposium on Quality of Service (IWQoS) | 979-8-3503-5012-8/24/$31.00 ©2024 IEEE | DOI: 10.1109/IWQoS61813.2024.10682934

***Abstract*—Integrated Sensing and Communication (ISAC) has been witnessed to be a new paradigm of wireless sensing in 5G networks. Users can benefit from pervasive sensing applications in various scenarios with no communication penalty. Given the diverse demands for sensing resources across different sensing tasks, elastic resource scheduling becomes crucial, particularly when resources are constrained. However, existing approaches often treat users equally, limiting their applicability in dealing with diverse sensing tasks in the real world. In this paper, we introduce ELASE, a pioneering sensing technique that enables real-time elastic scheduling of sensing resources. At the core of ELASE is the exploration of the user's state to precisely determine the sensing resource requirements and schedule resources accordingly. We build the first model for matching sensing resources with sensing demands, and further propose a predictive scheduling scheme to eliminate delays by leveraging the 5G virtualized radio access network (vRAN). We conduct experiments to evaluate the performance of ELASE under different settings. The results demonstrate that ELASE outperforms the non-scheduling scheme, with a 34% reduction in trajectory tracking error and a 92% decrease in resource allocation error.**

***Index Terms*—5G vRAN, RF Sensing, Resource Scheduling**

I. INTRODUCTION

Due to the contact-less, privacy-protection, and even battery-free features, wireless sensing technologies have achieved great progress in the past few years. The mainstream radio frequency (RF) based wireless sensing has exploited wireless signals at various frequencies, ranging from LoRa [1], [2], RFID [3], [4], Wi-Fi [5]–[11] to mmWave [12], [13].

Although these works have demonstrated the feasibility of wireless-sensing applications, the method of deploying specific devices prohibits wide-range popularization. The concept of ISAC proposed in mobile networks can solve the problem by building sensing system upon the pervasive base stations [14], [15]. Despite the pervasiveness, another useful feature of mobile networks is the centralized RF resource scheduling. Wi-Fi and backscatter networks [16], [17] widely adopt mechanisms like the contention-based CSMA/CA and the deep coupling between preamble signals and data packets. This will produce an unstable sampling rate of the sensing signals due to either the resource contention among sensing targets or the lack of valid data packets. Differently, the centralized resource scheduling and the separation of data and control channels in the mobile network can offer a stable sampling rate of the sensing signals with less multi-target contention and no data-transmission dependency.

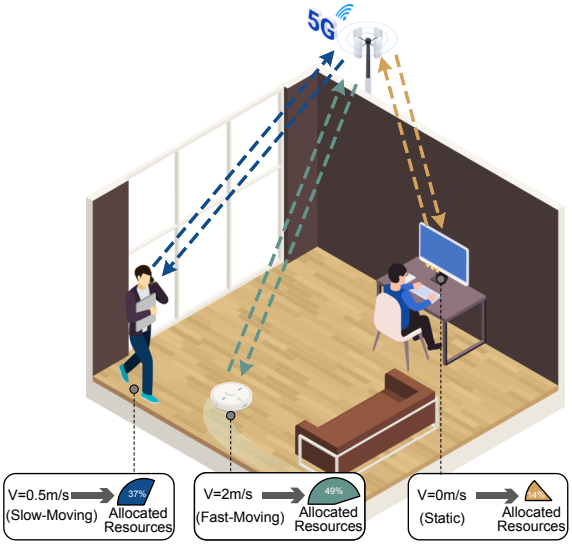

Fig. 1: Elastic Sensing with ELASE.

In existing ISAC works with 4G LTE and 5G NR [18]–[26], we find that the majority of them have considered reducing the sensing errors by applying advanced signal processing algorithms [18], [19], emerging artificial intelligence technologies [20], [21], multi-stream infrastructure (*e.g.*, multiple antennas [22] and multiple base stations [23]) when processing the LTE and NR reference signals (RS). However, lacking deep considerations of the intrinsic features of mobile networks, these topics are more or less discussed in other RF signal based works and similar solutions can be found.

We believe that the above-mentioned centralized resource scheduling is one of the intrinsic features to be well considered in ISAC. Take the existing works as an example, where fixed and averaged RS resources are shared among different UEs by default. Due to the limited total amount of available RS resources, one fast-moving UE will experience a sensing-quality degradation while there will be a waste of RS resources for the other static UEs. Since the RAN protocol stack integrates a data-plane scheduler that detects the data transmission demand of different UEs and schedules the limited data-plane resources among them under the principle of a long-term fairness, *can we design and integrate a similar*

† Yuan He is the corresponding author.

RS scheduler to simultaneously boost the sensing quality and reduce the resource waste in the multi-target sensing scenarios?

In traditional hardware-based black-box mobile networking infrastructure, only large device vendors can achieve this goal and efforts have to be spent on the hardware modification. Fortunately, the emerging 5G mobile networking technology named vRAN [27]–[30] offers a more flexible way to achieve the interoperation for ISAC. First, vRAN adopts the idea of Network Function Virtualization (NFV) and implements the RAN protocol stack on general processors instead of dedicated chips in software. This gives us the opportunity of deploying a dedicated RS scheduler and upgrading it on demand. Besides, vRAN specifies a group of standardized interoperation interfaces, which enables the dynamic service loading and parameter adjustment. Plenty of works have leveraged the white-box 5G vRAN to enhance the data-transmission services like the cross-layer optimized video streaming [31]–[34].

Though 5G vRAN shows promise in the wireless sensing applications, we have to tackle the following technical challenges before turning the above RS scheduler extension into a practical system:

- **First, how to match sensing demands with sensing resources?** Within the scope of our research, there is currently no work focusing on sensing resource scheduling in 5G networks. The criteria for estimating sensing resources, defining sensing demands, and matching them are not clear.
- **Second, how to eliminate scheduling delays?** We hope that the scheduler's resource allocation plan will change as soon as the demands of UEs change, but scheduling delays still exist inevitably. The scheduling delays come from the execution time of the state recognition algorithm and its requirement for recording some sampling points.

In this paper, we propose ELASE to address the above challenges. Our main contributions can be summarized as follows:

1) We discuss the feasibility of the RS scheduling with 5G vRAN and provide our considerations about the scheduling space and principles (Sec.II).
2) We dissect the architecture of ELASE and present its three main components named *UE state recognition*, *SRS resource scheduling* and *Elimination of scheduling delays*(Sec.III).
3) We implement ELASE with a 5G vRAN and commercial 5G UEs and conduct extensive evaluation experiments. The results show that ELASE can elastically schedule appropriate sensing resources for UEs in different environments and motion states, thus achieving small tracking errors. The predictive scheduling scheme can further reduce allocation errors for sensing resources. (Sec.IV).

Besides the above core contents, we also (i) discuss the limitations of ELASE and point out corresponding future directions in Sec.V, and (ii) summarize the related works and their differences with ELASE in Sec.VI. Finally, Sec.VII presents a conclusion of our work.

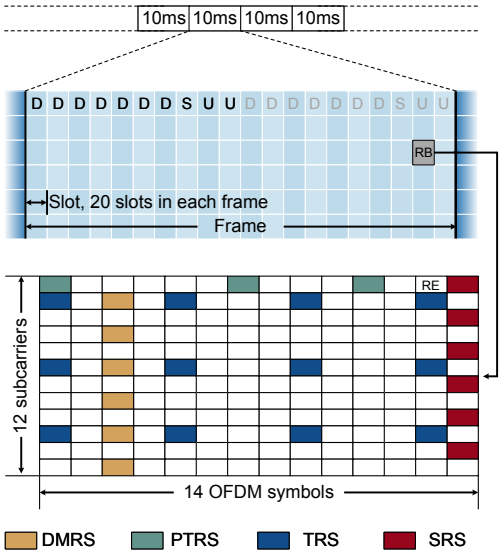

Fig. 2: 5G PHY frame structure and time-frequency domain patterns of four different reference signals in the U slot.

II. BACKGROUND

In this section, we first review the organization of the time-frequency domain resource in 5G. Then, we introduce the background of 5G vRAN and discuss the feasibility of elastically scheduling the sensing resource in 5G vRAN (Sec.II-B). Finally, we highlight the design principles of our elastic resource scheduler (Sec.II-C).

A. Organization of 5G Reference Signal

5G frame structure. 5G NR's physical layer (PHY) adopts the Orthogonal Frequency Division Multiplexing (OFDM) as the basic modulation scheme. As illustrated in Fig.2, the resource elements (REs) of 14 OFDM symbols in the time domain and 12 subcarriers in the frequency domain form the basic time-frequency unit named Resource Block (RB). The 5G slot is the time unit of one RB. Multiple continuous 5G slots are structured into 5G frames. Typically, one frame lasting 10 ms contains 20 slots with three different types: Downlink (D), Uplink (U) and Special (S). Fig.2 shows a basic slot format of "DDDDDDDSUU" in the commonly used Time Division Duplex (TDD) mode.

Different 5G reference signals. 5G NR adopts various types of reference signals for clock synchronization, frequency compensation and channel estimation for data transmission, including Tracking Reference Signal (TRS), Phase Tracking Reference Signal (PTRS) and Demodulation Reference Signal (DMRS) respectively. Moreover, for target sensing, it adopts the Channel State Information Reference Signal (CSI-RS) in the downlink channel and the Sounding Reference Signal (SRS) in the uplink channel. Our system utilizing 5G vRAN for elastic sensing only focuses on processing the continuous samples of SRS. Different reference signals have different

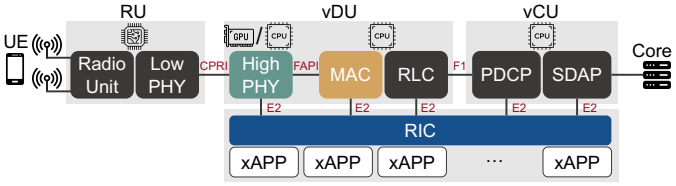

Fig. 3: Protocol stack of 5G vRAN: key modules run on general-purpose processors and interconnect with each other through standardized interfaces.

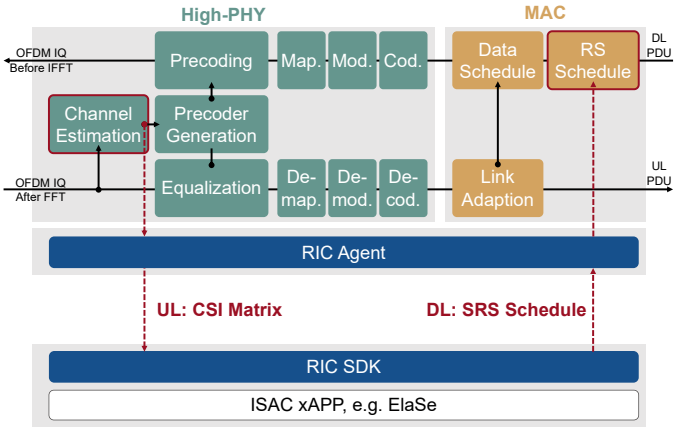

Fig. 4: Feasibility of manipulating 5G SRS: obtaining CSI from the channel estimation module in PHY and issuing elastic SRS allocation to the RS scheduler in MAC.

time-frequency patterns regulated by the standards. We depict a classic case of these patterns in Fig.2, where SRS REs appear in the 14th OFDM symbol with a subcarrier spacing of 2 (termed as comb2 in 5G).

B. Manipulating SRS for Sensing in 5G vRAN

Basic information of 5G vRAN. 5G vRAN is proposed to solve the closedness problem of the traditional RAN based on ASIC chips.

Fig.3 shows the typical data-plane structure of the 5G vRAN protocol stack, from bottom to top including PHY layer, Medium Access Control (MAC) layer, Radio Link Control (RLC) layer, Packet Data Convergence Protocol (PDCP) layer and Service Data Adaptation Protocol (SDAP) layer. Since RLC, PDCP and SDAP are mainly responsible for the data transmission like packet retransmission, segmentation, security and quality-of-service enhancement, etc., we here mainly review the details of PHY and MAC.

In 5G vRAN, PHY layer is separated into two parts: (i) the low PHY responsible for relatively fixed signal processing functions like FFT and iFFT; (ii) the high PHY responsible for upgradable modules like channel estimation, OFDM modulation and channel coding.MAC layer centrally schedules physical resources for data transmission, reference signals, and broadcast signals. To integrate 5G vRAN with the capability of ISAC, we mainly focus on PHY's channel estimation module for the CSI retrieving and MAC's scheduler module for the elastic SRS scheduling.

Feasibility of on-demand SRS manipulating with RIC. The software-implemented protocol stack of 5G vRAN gives

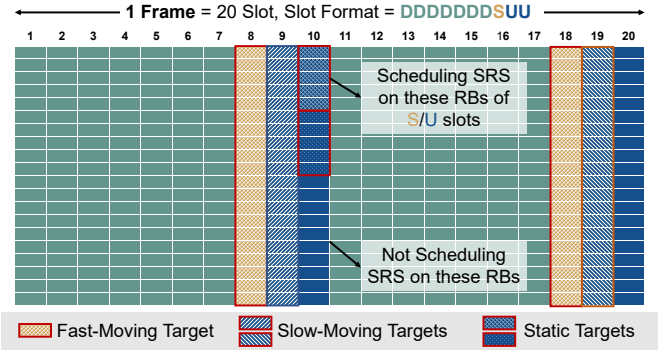

Fig. 5: Example of SRS scheduling for multiple targets: faster target has more SRS resources in time domains.

us the opportunity of manipulating SRS signals. Moreover, the O-RAN alliance [35] has proposed the RAN Intelligence Control (RIC) as the standardized interfaces for the vRAN interaction [36]. To obtain real-time information from vRAN and perform intelligent control, the customized xApps built with the RIC SDK interact with the RIC agent embedded in the vRAN via the E2 protocol. Although the current E2 protocol does not directly support the functionality of the SRS manipulation, we can easily conduct such extension based on its various implementations [37]. As depicted in Fig.4, with the help of RIC, an xApp designed for the ISAC application can deliver the SRS schedule to the MAC layer's RB scheduler and collect the estimated channel parameter to form the complete CSI matrix.

C. ELASE's Scheduling Principles of 5G SRS.

Before digging into the detailed designs of ELASE, we introduce our basic considerations in the SRS scheduling pattern, range, and logic. For a typical setting of the "DDDDDDDSUU" slot format, SRS can be scheduled in the S and U slots. For the typical 100 MHz bandwidth in 5G, each slot has 273 RBs in the frequency domain. To provide a more effective SRS scheduling, we adopt the following principles:

Scheduling Pattern: First, for the SRS comb pattern, we choose the default *comb2* instead of other available options such as *comb4*. Second, for the SRS symbol pattern, we adopt at most one SRS symbol in each slot. The rationale behind our selections is the trade-off between the gain and cost: obtaining a denser CSI sample in one slot yields a limited sensing gain. Third, we choose continuous RB allocation each schedule instead of the dispersed one, *i.e.,* allocating [*RB_start*, *RB_num*] for each user at each slot. According to the 5G NR standard, the value of *RB_start* can be arbitrary while the value of *RB_num* must be chosen from the non-contiguous values in a predefined table (Table 6.4.1.4.3-1 of 3GPP TS38.211 [38]). It's worth noting that the maximum value of *RB_num* is 272 instead of 273 because the number needs to be a multiple of 4.

Scheduling Range: Here we mainly discuss the sparsest schedule and the densest schedule of SRS RBs in the time-frequency domain. For the sparsest one, we comply with the reference implementation of a most popular vRAN system

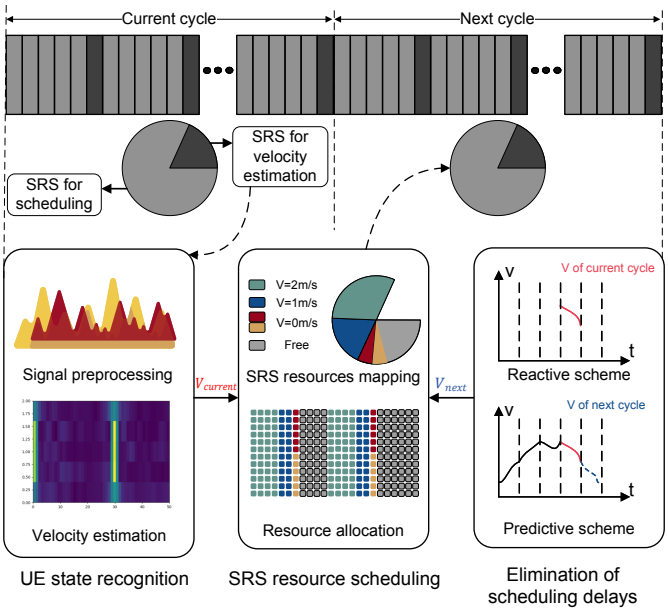

Fig. 6: Design overview of ELASE.

named OAI [28] where at least four SRS RBs of one 5G frame are scheduled for one UE. For the most densest one, we allocate 272 RBs within one 5G slot to one UE in each half 5G frame (also called one subframe). We only allocate at most one slot in the three consecutive S/U slots to one target, mainly because more consecutive slot allocations cannot effectively increase the sampling frequency. Fig.5 illustrates an example where we allocate all RBs in slot 8 and slot 18 to a fast-moving object.

III. SYSTEM DESIGN

A. ELASE *Overview*

The overview of ELASE is shown in Fig.6. ELASE implements a real-time system for identifying UE's state and scheduling SRS sensing resources. We introduce each module below:

• **UE state recognition.** ELASE aims to accurately identify the dynamic demands of UEs of sensing resources. To achieve this objective, we leverage the UE's velocity as a state indicator, recognizing that different velocities reflect different states and require varying SRS resources. To determine the UE's velocity, we utilize the existing low sampling rate SRS available in communication and derive the velocity information from the CSI. It is important to note that the velocity estimation algorithm requires a certain number of sampling points, and frequent estimations will result in significant computational overhead. To address this, we implement a periodic strategy and find out the appropriate cycle length.

• **SRS resource scheduling.** After determining the UE's state, the allocation of SRS resources to each UE becomes necessary. We categorize UEs into two states: stationary and moving, and assign different SRS bandwidths to each state. Additionally, we map the UE's velocity to corresponding SRS sampling rates. Once the UE's velocity is mapped to SRS resources (SRS bandwidths and sampling rates), the base station is responsible for scheduling the SRS transmission to UEs in different time slots. ELASE converts the scheduling problem into a resource allocation problem aimed at minimizing the number of required time slots.

• **Elimination of scheduling delays.** The velocity of each UE is calculated by the base station at the end of each cycle. One intuitive approach is to employ an immediate response scheduling strategy, where the current velocity is utilized to allocate sensing resources for the next cycle. We call it Reactive Scheduling Scheme. However, this scheme introduces a significant delay between the UE acquiring sensing resources and its state change when the UE's velocity changes. To eliminate delays, we perform a delay analysis and propose a Predictive Scheduling Scheme.

• **Multi-target sensing.** Finally, ELASE accomplishes different sensing tasks using the different amounts of SRS resources scheduled to different targets. In this context, we consider localization and tracking as multi-target sensing tasks.

B. *UE State Recognition*

In Sec.II-C, we mentioned that in the original 5G communication system, each frame assigns one SRS for channel quality estimation. This SRS has a sampling rate of 100 Hz. We utilize this periodic SRS to identify the UE's velocity. We introduce the velocity estimation algorithm in this section.

1) Velocity Estimation Algorithm: Prior researches [39]–[41] have proposed methods for estimating the velocity of device movement using CSI exclusively. This method proposed by C^2IL [39] is based on the electromagnetic standing wave field. C^2IL finds through electromagnetic wave propagation theory and measurements that when an antenna traverses an indoor space at a velocity of v, a periodically ripple-like pattern with a frequency of f_0 emerges, following the relationship $f_0 = \frac{2*v}{\lambda}$, where λ represents the wavelength of the electromagnetic wave. C^2IL utilizes a CSI matrix over time on one spatial stream and one subcarrier to extract the frequency f after undergoing data preprocessing, noise cancellation, fading enhancement, and frequency estimation. By extracting f from multiple subcarriers and selecting the median value f_0 as the final result. Then the moving velocity is estimated by:

$$v = \frac{\lambda * f_0}{2} \tag{1}$$

2) Periodic Strategy: The velocity estimation algorithm requires a certain number of sampling points. However, adopting a pipeline strategy would introduce significant computational overhead. Considering the need for resource scheduling, we adopt a periodic strategy. At the end of each cycle, the base station calculates the velocity of the UE in the current cycle and schedules the SRS resources for the next cycle. If the cycle is set too short, there would not be enough CSI samples to identify the UE's state, and the scheduling space for the next cycle would be insufficient. On the other hand, if the cycle is set too long, the estimated average velocity

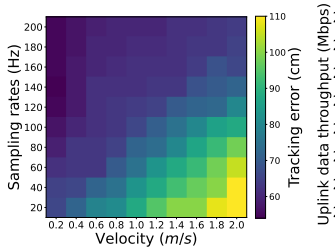

Fig. 7: Variant tracking errors under different velocities and sampling rates.

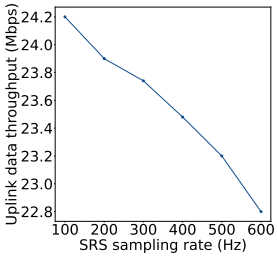

Fig. 8: Uplink data throughput using SRS with different time slot numbers

of the UE in the current cycle could not represent the UE's state accurately, leading to inadequate real-time performance of the system. We will measure the impact of different cycle lengths on resource scheduling in our experiments.

Furthermore, ELASE minds real-time sensing resource scheduling, taking into account the time consumed by the velocity estimation algorithm and resource allocation algorithm. Our measurements show that these tasks can be completed in less than 20 ms, which is negligible compared to the cycle length.

C. SRS Resource Scheduling

1) Mapping Velocity to SRS Resources: After obtaining the velocity of each UE, it is necessary to convert the velocity into sensing resource demand. Initially, we classify UEs into two states: stationary and moving. Recognizing that dynamic tracking necessitates a greater bandwidth compared to static localization, we allocate half bandwidth to stationary UEs and all bandwidth to moving UEs. Then, let's delve into the determination of the sampling rate. According to [39], the typical velocity of walking indoors ranges from 0.8 to 1.6 m/s, with a maximum value of 2 m/s. The velocity value represents the displacement of the UE per unit time, while the sampling rate represents the number of samples taken within the same unit of time. Assuming the UE is sampled once after the same displacement, we establish a positive correlation between the sampling rate and velocity value. Let's denote the sampling rate as f_s, the scaling coefficient as k, and the velocity value as v. The relationship among them can be expressed as follows:

$$fs = k * v \tag{2}$$

To determine the coefficient k, we conduct a set of pre-experiments to measure the relationship between tracking error and sampling rate. We set the velocities of UE from 0 m/s to 2 m/s, and the sampling rate from 20 Hz to 200 Hz. We use the sampling method when the rate is less than the sparsest rate and keep the bandwidth of SRS 100 MHz. The localization method adopts a modified super-resolution method from SpotFi [42]. The experimental results are shown in the Fig.7. Based on the experimental findings, we determine the value of the scaling coefficient as k=100 to keep the average trajectory tracking error less than 70 cm.

Additionally, for UEs with extremely low velocities, it is essential to maintain a minimum SRS sampling rate. Therefore, we have set a threshold of 50 for the minimum sampling rate. To summarize, the sampling rate is given by:

$$fs = \begin{cases} 50 & , v \leq 0.5m/s \\ 100 * v & , v > 0.5m/s \end{cases} \tag{3}$$

2) Resource Allocation Algorithm: Once the demands of SRS resources for the next cycle are determined, the base station considers scheduling which SRS resources in the time and frequency dimensions for each UE. This resource allocation problem can be transformed into a two-dimensional coloring problem. In the time domain, there are 500 time slots per second available for SRS resources, while in the frequency domain, a bandwidth of 272 RBs is allocated. It is possible to divide and allocate bandwidth to different UEs within the same time slot, but the allocated bandwidth for a single UE remains continuous.

Effects of SRS slot numbers on data throughput. We conduct experiments to measure the uplink data throughput when using SRS with different time slot numbers. Fig.8 demonstrates that the uplink data throughput decreases as SRS slot numbers increase. The throughput with 600 SRS slot numbers exhibits a 5.8% decrease compared to that with 100. Sensing resources and communication resources are mutually exclusive in the OFDMA structure.

Therefore, to minimize the total number of SRS time slots, the resource allocation algorithm combines the sensing resource demands of all UEs. If the combined SRS bandwidth required by multiple UEs does not exceed 100 MHz, they can be merged into a single time slot. In our resource mapping scheme, two stationary UEs can each occupy 50 MHz bandwidth within the same time slot. It is important to note that different resource mapping schemes may exist, allowing for a finer distinction of UE SRS bandwidth requirements. In such cases, multiple UE SRSs with a total bandwidth not exceeding the upper limit can be allocated in the same time slot.

In scenarios where the total SRS resource demands exceed the upper limit, our allocation algorithm prioritizes UEs based on their velocities. Resources are assigned to UEs with larger velocities until the remaining resources are insufficient. However, alternative methods can also be employed for different application scenarios. Here we provide the following two examples:

1) **Priority-based approaches:** The base station can calculate the priority of resource allocation for UEs based on other conditions. For example, it can compute the sum of resources allocated to UEs in the past several cycles, where lower sums indicate higher priority.
2) **Proportional fair approaches:** Proportional fairness is widely used in scheduling algorithms in different fields. The base station reduces the sensing resources allocated to each UE in the same proportion when the demands exceed the upper limit.

TABLE I: A scenario where UE accelerates first and then moves uniformly. Predictive Scheduling Scheme eliminates the scheduling delay.

Cycle	1	2	3	4	5	6
UE's acceleration	Zero	Positive	Positive	Zero	Zero	Zero
UE's velocity	Zero	Low	Low	High	High	High
Reactive scheme	\	Recognize velocity in 2	Recognize velocity in 3	Recognize velocity in 4	Schedule a high sampling rate SRS	\
Predictive scheme	\	Predict velocity in 3	Predict velocity in 4	Schedule a high sampling rate SRS	\	\

D. Elimination of Scheduling Delays

1) Reactive Scheduling Scheme: The Reactive Scheduling Scheme functions effectively when the UE's velocity remains constant. However, when the UE experiences changes in velocity, such as acceleration, the velocity in the next cycle exceeds the estimated velocity in the current cycle. Consequently, the sensing resources allocated based on the current cycle's velocity may prove insufficient to meet the actual demand. This scheme introduces a delay of one cycle between the change in the UE's velocity and the adjustment of allocated sensing resources. When considering resource allocation as a service to meet evolving demands over time, such delays can pose challenges for subsequent sensing applications.

The reason behind the one-cycle delay in the Reactive Scheduling Scheme is that the base station requires one cycle to obtain CSI for determining the UE's velocity. Therefore, when scheduling sensing resources for the UE in the next cycle, the UE's velocity in that cycle remains unknown. In response to this challenge, we propose the Predictive Scheduling Scheme.

2) Predictive Scheduling Scheme: Although the base station lacks knowledge of the UE's velocity in the next cycle during resource scheduling, it can gather historical velocity data of the UE in multiple past cycles. By utilizing this historical data, the base station can compute the current acceleration of the UE and use it to estimate the UE's velocity in the next cycle. Furthermore, to enhance the accuracy of UE velocity prediction, we employ a Kalman filter that combines prior information with measurement information. This integrated approach enables more precise state estimation. The velocity prediction algorithm leverages the acceleration values and Kalman filtering to predict the velocity in the next cycle. At the end of the next cycle, the velocity estimation results are fed back into the filtering algorithm. This iterative process aims to continuously optimize the prediction algorithm and enhance its accuracy in predicting. By incorporating this feedback mechanism, the prediction algorithm can rectify and improve its predictions based on actual observed velocity data.

Table I illustrates the difference between the Reactive Scheduling Scheme and the Predictive Scheduling Scheme. In the scenario described, a UE remains stationary during the first cycle, accelerates from the 2nd to the 3rd cycle, and moves rapidly from the 4th to the 6th cycle. As the UE's velocity is high in the 4th cycle, it should ideally obtain a high sampling rate SRS during that cycle. However, due to the inherent delay of the Reactive Scheduling Scheme, the base station only recognizes the UE's velocity increase in the 4th cycle, causing the UE to obtain the high sampling rate SRS in the subsequent cycle. In contrast, the Predictive Scheduling Scheme predicts the velocity of the next cycle in the 3rd cycle, thereby eliminating scheduling delays.

E. Multi-target Sensing: Localizing and Tracking

After the resource scheduling process, the base station extracts CSI from the received SRS, analyzing it to determine the UE's serial number, time slot, and associated frequency. Leveraging this information, the base station can offer customized sensing applications for individual users. In ELASE, we take localizing and tracking as sensing tasks. We adopt and modify the localization algorithm from SpotFi. SpotFi utilizes the value of Received Signal Strength Indicator to estimate the distance, but we utilize the CSI amplitude. Besides, ELASE samples densely in the time domain. So we employ the continuity of movement to discard outliers and minimize localization errors.

IV. IMPLEMENTATION AND EVALUATION

A. Implementation

First, we build a complete 5G testbed including a 5G base station and multiple commercial 5G UEs. The 5G base station consists of the 5G vRAN and the 5G core network. Details of these components are listed as follows:

- **5G vRAN:** We adopt the most widely deployed open-sourced vRAN project named OpenAirInterface (OAI) [28]. The hardware-based RU of OAI runs a USRP N310 with 2 TX antennas and 2 RX antennas. The software-based vDU and vCU of OAI run on a PC equipped with an i9-13900K CPU and 16GB RAM. The USRP and the PC are connected through a 10 GBE optic fiber due to the heavy traffic of the raw IQ samples.
- **5G core network:** We deploy the commercial version of free5GC [43] for its better stability and easier operation than the open-sourced one. Since ELASE requires the raw CSI samples for a better sensing quality, we do not use the Location Management Function (LMF) provided by the 5G core. The core network runs on a Linux industrial computer directly connected to the vRAN PC with a 2.5 GBE network cable.
- **5G UEs:** We choose the commercial 5G Customer Premise Equipment (CPE) instead of the smartphone because it can access the private 5G network in non-public network frequency

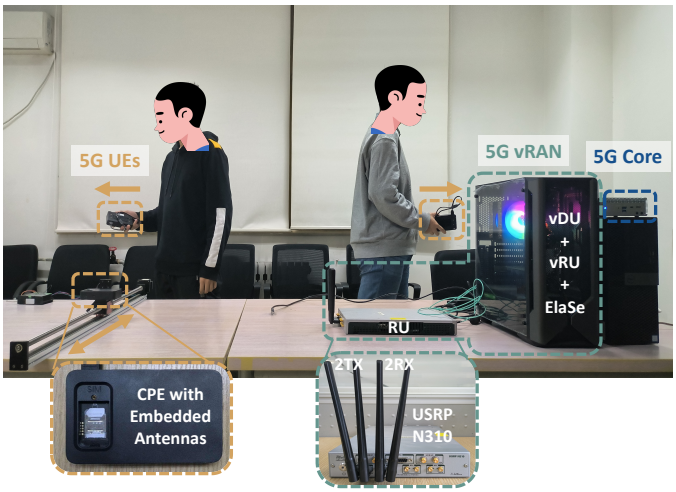

Fig. 9: Experiment scenario

bands like N77. No hardware and software modifications are applied to these UEs in ELASE.

Second, we implement the three key components of ELASE and deploy them on the same PC that hosts the OAI's protocol stack.

B. Baselines and Comparison Methodologies

The baseline is a scheme that uses the original SRS with a sampling rate of 100 Hz and a whole bandwidth, evenly allocated to UEs. We compare the baseline with two other scheduling schemes: reactive scheme and predictive scheme.

We use trajectory tracking error and resource allocation error as the metrics for evaluation. The trajectory tracking error measures the end-to-end performance of ELASE. The resource allocation error is defined as the absolute difference between the number of SRS allocated to one UE and the real demand in one cycle. The number of SRS is derived by multiplying the number of RBs by the number of slots. We use resource allocation error as the metric because ELASE focuses on elastic and real-time sensing resource scheduling. Besides, if the delay in scheduling increases, the value of allocation error will be larger.

C. Overall Performance

Trajectory tracking error. We first evaluate ELASE's performance of trajectory tracking in various environments, as illustrated in Fig.10. Three representative indoor scenarios are selected for testing purposes: 1) a meeting room with few multipath effects (5m×4.2m); 2) a narrow corridor(5m×2m); 3) a laboratory with rich multipath effects (5m×4m).

During each experiment, we connect three UEs to the base station and adopt the predictive scheduling scheme. Fig.10(a)(b)(c) depicts the system's tracking trajectory of UEs in these three environments, compared with the ground truth. Additionally, Fig.10(d) presents the cumulative distribution function (CDF) of the tracking error. It is evident that the laboratory environment showcases the highest tracking error, as indicated in Fig.10(c), mainly attributed to the heavy multipath. In the meeting room, corridor, and laboratory, the median trajectory tracking error is 60.24 cm, 63.57 cm, and 78.31 cm, respectively.

In the baseline scheme, the median trajectory tracking error is 90.25 cm, 94.53 cm, and 110.69 cm respectively. The median trajectory tracking error of ELASE in the predictive scheme is 34% lower than that of the baseline scheme.

Resource allocation error. Then we evaluate the performance of our allocation scheme under different motion states of UEs. The acceleration and velocity of UEs vary in different motion states. We analyze ELASE's performance of resource allocation in a 10-second motion of each UE.

Fig.11(a)(b)(c) illustrate the real demand for SRS by the three UEs and the changes in allocation over time in reactive, predictive, and baseline schemes. By comparing the real demand with the reactive scheme, we observe that the allocation results of the reactive scheme are generally close to the real demand in the previous cycle. This indicates a scheduling delay in the reactive scheme. In Fig.11(a), when the UE's velocity changes most of the time, it is evident that the allocation curve of the reactive scheme lags behind the real demand. However, in Fig.11(b), when the UE's velocity remains unchanged, the results of the reactive scheme align with the real demand value.

Fig.11(d) provides statistical results of the resource allocation error of the three schemes. The resource allocation error of the reactive scheme is 78% lower than that of baseline scheme, furthermore, the resource allocation error of the predictive scheme is 92% lower than that of baseline scheme. This is because the baseline scheme does not consider the state changes of the UE, resulting in insufficient sensing resources being allocated to the UE. The results illustrate that the prediction algorithm effectively predicts the velocity of the UE in the next cycle.

D. Impacting Factors

In order to comprehensively evaluate the performance of the system, we have identified some internal and external factors that affect it. Internal factors include the length of the scheduling cycle and the length of the prediction window, which affect the accuracy of UE state recognition and velocity prediction. External factors include the velocity and acceleration of UE motion, which have an impact on trajectory tracking.

Length of the scheduling cycle. We set different cycle lengths while keeping the UE's motion state the same. We normalize the resource allocation error in one cycle to obtain the allocation error in one second. The experimental results are presented in Fig.12(a).

For the reactive scheduling scheme, the resource allocation error initially decreases and then increases as the cycle length grows, reaching its minimum value at a cycle length of 0.4 seconds. When the cycle length is short, there are insufficient sampling points for state recognition, leading to inaccurate velocity calculation. Besides, when the cycle spans a longer duration, the recognition result is the average velocity during

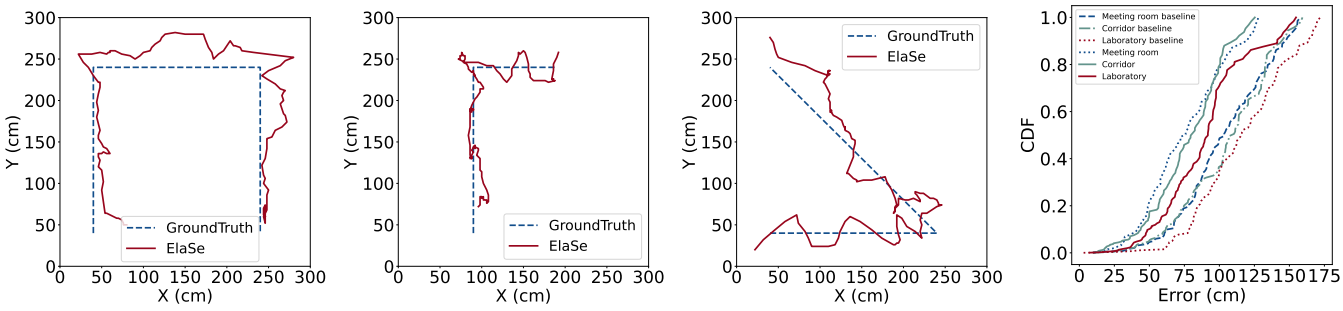

(a) Meeting room (b) Corridor (c) Laboratory (d) TE analysis

Fig. 10: Overall performance of trajectory tracking error in different environments.

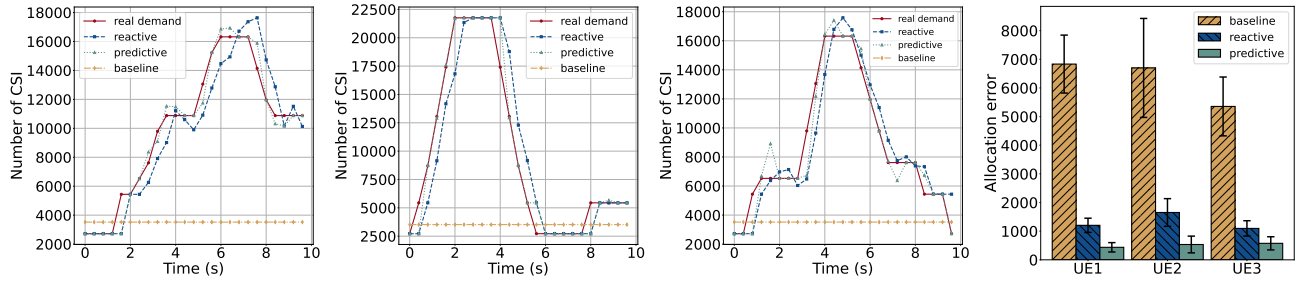

(a) UE 1 (b) UE 2 (c) UE 3 (d) AE statistic

Fig. 11: Overall performance of resource allocation error in different motion states.

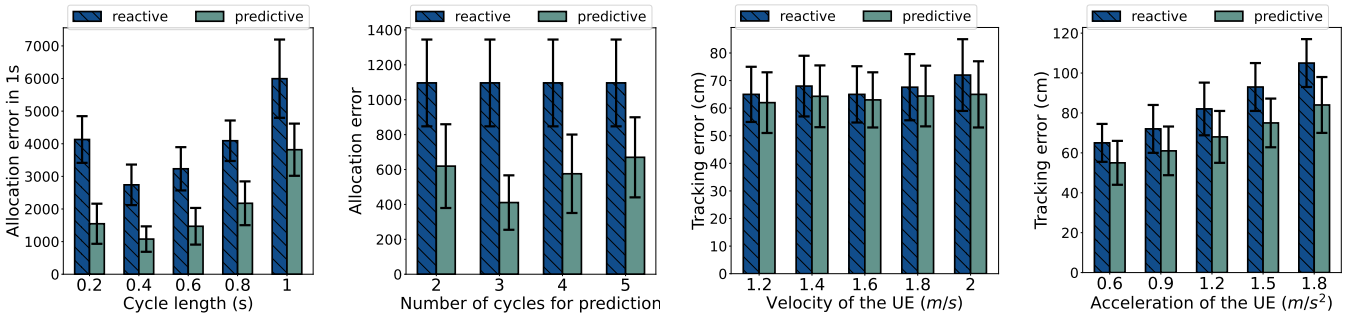

(a) Length of the scheduling cycle (b) Length of prediction window (c) UE velocity (d) UE acceleration

Fig. 12: Evaluation of the four main factors' impacts on the performance of ELASE.

past period, which causes resource allocation error because the UE may change state in one long cycle.

Length of the prediction window. We evaluate the impact of the length of the prediction window on allocation error. A smaller resource allocation error indicates more accurate velocity prediction. We set the cycle length to 0.4 seconds and vary the length of the prediction window from 2 cycles to 5 cycles in our experiments. The results are shown in Fig.12(b).

The resource allocation error of the reactive scheme is not affected by the prediction window length and remains consistent. For the predictive scheme, the resource allocation error is minimized when the prediction window length is 3 cycles. This suggests that in the experimental scenario, there is the highest correlation between the UE's motion and its motion state within the previous 1.2 seconds. Using more historical velocity data, on the other hand, can decrease the accuracy of the prediction.

Velocity of UEs. We select the optimal parameter values for the following experiments. The length of the scheduling cycle is set to 0.4 seconds, and the prediction window length is three cycles. We further evaluate the influence of UE's velocity on tracking error. The UE's velocity range is set from 1.2 m/s to 2 m/s with an interval of 0.2 m/s. We analyze the process of uniform motion and present the results in Fig.12(c). As the UE's velocity increases, the trajectory tracking error remains relatively constant. This observation illustrates that the system's scheduling scheme ensures the stability of trajectory tracking error by allocating more sensing resources to high-speed UEs.

Acceleration of UEs. We set the UE to speed up from 0 m/s to 2 m/s with different accelerations and analyze the trajectory tracking error during the acceleration process. The results are shown in Fig.12(d). As the UE's acceleration increases, both reactive and predictive schemes show an increase in tracking

error, with the increase being more gradual in the predictive scheme. The reactive scheme has a scheduling delay of one cycle. Therefore, as the UE's acceleration increases, the delay leads to an increase in tracking error. The predictive scheme can better adapt to motion with a constant acceleration.

V. Discussion and Future Works

In this section, we discuss practical issues concerning the applicability and efficacy of ELASE and propose corresponding future research directions.

A. Applying ELASE to other sensing cases

In the cases of localization and tracking, velocity is considered as an effective metric for describing the dynamic demands of UEs. However, not all cases can apply velocity as a general metric. For example, in gesture recognition or fall detection, the spectral characteristics of the target have been proven to be an effective indicator. In system design, we particularly pay attention to this point and decouple the user state recognition and SRS resource scheduling modules by using reference signals in different time slots. This loose coupling ensures the effectiveness of resource scheduling and also provides flexibility for choosing new metrics when applying ELASE to other sensing cases.

B. Combining Multi-stream 5G Reference Signals for a Better Sensing Quality.

First, ELASE uses the uplink SRS signals only mainly because of the inaccessibility of the CSI processing module of the commercial 5G UEs. The first category of extension is to utilize the uplink DMRS. Since that the DMRS symbols only experience one more layer of precoding than the SRS symbols, successive works can convert the DMRS-based CSI into the SRS-based CSI and extend the total amount of sensing resources. Besides, successive works can utilize the link symmetricity and use the downlink CSI-RS and DMRS signals provided by white-box UE devices for the further extension. Note that such multi-stream extensions are quite straightforward to be implemented in ELASE with our defined scheduling interface and logic. Challenges like handling the dynamics caused by the binding between DMRS to data streams and quantifying the quality of multi-channel sensing signals before the integration need to be further addressed.

VI. Related Works

A. Wireless Sensing with LTE/5G

Nowadays, ISAC with LTE and 5G has attracted growing research attention. Many works model the localization errors, discuss the impacts of modulation methods and sensing algorithms on the errors, and conduct extensive simulation-based evaluations [14], [15], [44]. Besides, Feng *et al.* propose the interference cancellation [19] and the noise reduction [18] algorithms to address the practical issues when applying traditional signal processing based solutions like AoA/DoA in real-world applications like the pedestrian tracking. Except for improving traditional algorithms, several works utilize classic machine learning algorithms and emerging deep learning algorithms to further reduce the sensing errors [21] and defend the replay attacks [20]. Last, recent innovations in the sensing infrastructure like the uniformed linear array antenna [22], the multi-cell RS integration [23] and multi-source RS integration [45] manage to bring the ISAC's capability to a new level.

Although these works have tried their best to reduce the sensing errors and some have claimed the feasible extension in the multi-target sensing scenarios, they only use the vanilla RS signals with default settings. This priori condition hinders them from offering fairness among the targets when the RS resources are very limited. Different from them, ELASE dynamically recognizes the resource demand of different targets and elastically schedules the limited RS resources among them, which is in parallel with the related advances in the algorithm optimization and the infrastructure upgrading.

B. Multi-target Wireless Sensing

Various wireless signals exhibit the ability to sense multiple targets simultaneously, such as WiFi signals [46]–[48], acoustic signals [49]–[52], mmWave signals [13], [53] and so on. WiPolar [47] leverages the different polarization of reflected signals to accurately separate the multipaths from different targets, which, in turn, allows it to track them simultaneously. Symphony [50] exploits the layout of the microphone array to distinguish acoustic signals from different targets along different paths as well as signals from the same target, then calculates their locations concurrently.

Despite their inspiring abilities of sensing multiple targets, all usable resources (*e.g.,* frequency) are employed in the existing works without a resource allocation mechanism. In contrast, ELASE elastically allocates sensing resources among the multiple targets to achieve better scalability.

VII. Conclusion

In this paper, we present the first sensing resource scheduler in 5G networks, ELASE, to schedule SRS resources for UEs elastically and in time. ELASE benefits from the programmability of 5G vRAN and utilizes the interface of its protocol stack. It uses the velocity of UEs to represent the time-variant sensing demands. ELASE saves sensing resources by minimizing the number of used sensing slots to preserve communication capabilities. It adopts a predictive scheduling scheme to eliminate scheduling delays. Extensive experiments under real-world scenarios show that ELASE can schedule sensing resources appropriately in different situations, achieving small trajectory tracking errors and resource allocation errors.

VIII. Acknowledgement

We thank our anonymous shepherd and reviewers for their insightful comments. This research was supported by the National Natural Science Foundation of China (U21B2007, 62325203, and U22B2033) and Alibaba Innovative Research (No. 2021010286).

REFERENCES

[1] B. Xie, Y. Yin, and J. Xiong, "Pushing the Limits of Long Range Wireless Sensing with LoRa," *Proceedings of ACM IMWUT*, 2021.

[2] H. Jiang, J. Zhang, X. Guo, and Y. He, "Sense Me on the Ride: Accurate Mobile Sensing over a LoRa Backscatter Channel," in *Proceedings of ACM Sensys*, 2021.

[3] Z. Luo, Q. Zhang, Y. Ma, M. Singh, and F. Adib, "3D Backscatter Localization for Fine-Grained Robotics," in *Proceedings of USENIX NSDI*, 2019.

[4] B. Liang, P. Wang, R. Zhao, H. Guo, P. Zhang, J. Guo, S. Zhu, H. H. Liu, X. Zhang, and C. Xu, "RF-Chord: Towards Deployable RFID Localization System for Logistic Networks," in *Proceedings of USENIX NSDI*, 2023.

[5] E. Soltanaghaei, A. Kalyanaraman, and K. Whitehouse, "Multipath Triangulation: Decimeter-Level WiFi Localization and Orientation with a Single Unaided Receiver," in *Proceedings of ACM MobiSys*, 2018.

[6] X. Zheng, K. Yang, J. Xiong, L. Liu, and H. Ma, "Pushing the Limits of WiFi Sensing with Low Transmission Rates," *IEEE TMC*, 2024.

[7] X. Zheng, J. Wang, L. Shangguan, Z. Zhou, and Y. Liu, "Design and Implementation of a CSI-Based Ubiquitous Smoking Detection System," *IEEE/ACM Transactions on Networking*, 2017.

[8] T. Hang, Y. Zheng, K. Qian, C. Wu, Z. Yang, X. Zhou, Y. Liu, and G. Chen, "WiSH: WiFi-Based Real-Time Human Detection," *Tsinghua Science and Technology*, 2019.

[9] X. Zou, J. Liu, J. Han, W. Xi, and Z. Wang, "WiHunter: Enabling Real-time Small Object Detection via Wireless Sensing," in *Proceedings of IEEE/ACM IWQoS*, 2023.

[10] G. Yu, M. Wang, P. Zhao, Y. Wang, H. Zhou, Y. Ji, and C. Wu, "SpiroFi: Contactless Pulmonary Function Monitoring using WiFi Signal," in *Proceedings of IEEE/ACM IWQoS*, 2022.

[11] Y. Sun, Y. He, J. Zhang, X. Na, Y. Chen, W. Wang, and X. Guo, "BIFROST: Reinventing WiFi Signals Based on Dispersion Effect for Accurate Indoor Localization," in *Proceedings of ACM SenSys*, 2023.

[12] C. Jiang, J. Guo, Y. He, M. Jin, S. Li, and Y. Liu, "mmVib: Micrometer-Level Vibration Measurement with mmWave Radar," in *Proceedings of ACM MobiCom*, 2020.

[13] J. Zhang, X. Na, R. Xi, Y. Sun, and Y. He, "mmHawkeye: Passive UAV Detection with a COTS mmWave Radar," in *Proceedings of IEEE SECON*, 2023.

[14] Z. Wei, H. Qu, Y. Wang, X. Yuan, H. Wu, Y. Du, K. Han, N. Zhang, and Z. Feng, "Integrated Sensing and Communication Signals Towards 5G-A and 6G: A Survey," *IEEE IoTJ*, 2023.

[15] R. Keating, M. Säily, J. Hulkkonen, and J. Karjalainen, "Overview of Positioning in 5G New Radio," in *Proceedings of IEEE ISWCS*, 2019.

[16] X. Na, X. Guo, Y. He, and R. Xi, "Wi-attack: Cross-technology Impersonation Attack against iBeacon Services," in *Proceedings of IEEE SECON*, 2021.

[17] X. Na, X. Guo, Z. Yu, J. Zhang, Y. He, and Y. Liu, "Leggiero: Analog WiFi Backscatter with Payload Transparency," in *Proceedings of ACM MobiSys*, 2023.

[18] Y.Feng, Y.Xie, D.Ganesan, and J. Xiong, "LTE-Based Low-Cost and Low-Power Soil Moisture Sensing," in *Proceedings of ACM SenSys*, 2022.

[19] Y.Feng, Y.Xie, D.Ganesan, and J.Xiong, "LTE-Based Pervasive Sensing across Indoor and Outdoor," in *Proceedings of ACM SenSys*, 2021.

[20] K. Gao, H. Wang, H. Lv, and P. Gao, "Your Locations May Be Lies: Selective-PRS-Spoofing Attacks and Defence on 5G NR Positioning Systems," in *Proceedings of IEEE INFOCOM*, 2023.

[21] Z. Liu, L. Chen, X. Zhou, Z. Jiao, G. Guo, and R. Chen, "Machine Learning for Time-of-Arrival Estimation with 5G Signals in Indoor Positioning," *IEEE IoTJ*, 2023.

[22] M. Pan, P. Liu, S. Liu, W. Qi, Y. Huang, X. You, X. Jia, and X. Li, "Efficient Joint DOA and TOA Estimation for Indoor Positioning with 5G Picocell Base Stations," *IEEE TIM*, 2022.

[23] R. Peng, Y. Tian, and S. Han, "ICI-Free Channel Estimation and Wireless Gesture Recognition Based on Cellular Signals," *IEEE WCL*, 2023.

[24] X. Guo, Y. He, X. Zheng, L. Yu, and O. Gnawali, "ZigFi: Harnessing Channel State Information for Cross-Technology Communication," in *Proceedings of IEEE INFOCOM*, 2018.

[25] W. Wang, X. Zheng, Y. He, and X. Guo, "AdaComm: Tracing Channel Dynamics for Reliable Cross-Technology Communication," in *Proceedings of IEEE SECON*. IEEE Press, 2019.

[26] Z. XIAO and Y. ZENG, "An Overview on Integrated Localization and Communication Towards 6G," *SCIENCE CHINA Information Sciences*, 2022.

[27] "Intel FlexRAN," https://github.com/intel/FlexRAN, 2023/10/20.

[28] "Eurecom openairinterface," https://openairinterface.org/, 2023/10/20.

[29] A. Garcia-Saavedra and X. Costa-Perez, "O-RAN: Disrupting the Virtualized RAN Ecosystem," *IEEE Communications Standards Magazine*, 2021.

[30] G. Garcia-Aviles, A. Garcia-Saavedra, M. Gramaglia, X. Costa-Perez, P. Serrano, and A. Banchs, "Nuberu: Reliable RAN Virtualization in Shared Platforms," in *Proceedings of ACM Mobicom*, 2021.

[31] C. Baena, M. Hervás-Gutiérrez, E. Baena, J. Villegas, R. Barco, and S. Fortes, "Assessing the Impact of Computational Resources to the Quality of Experience Provided by vRANs," *IEEE Access*, 2023.

[32] B. Agarwal, M. A. Togou, M. Ruffini, and G.-M. Muntean, "QoE-Driven Optimization in 5G O-RAN-Enabled HetNets for Enhanced Video Service Quality," *IEEE Communications Magazine*, 2022.

[33] D. Xu, A. Zhou, G. Wang, H. Zhang, X. Li, J. Pei, and H. Ma, "Tutti: Coupling 5G RAN and Mobile Edge Computing for Latency-Critical Video Analytics," in *Proceedings of ACM MobiCom*, 2022.

[34] Y. Chen, R. Yao, H. Hassanieh, and R. Mittal, "Channel-Aware 5G RAN Slicing with Customizable Schedulers," in *Proceedings of USENIX NSDI*, 2023.

[35] "O-RAN Resources," https://www.o-ran.org/resources, 2023/10/20.

[36] "RIC specifications from O-RAN Alliance," https://orandownloadsweb.azurewebsites.net/specifications, 2023/10/20.

[37] R. Schmidt, M. Irazabal, and N. Nikaein, "FlexRIC: An SDK for Next-Generation SD-RANs," in *Proceedings of ACM CoNEXT*, 2021.

[38] "3GPP TS 38.211 Release 16," https://www.etsi.org/deliver/etsi_ts/138200_138299/138211/16.02.00_60/ts_138211v160200p.pdf, 2023/10/20.

[39] Z.-P. Jiang, W. Xi, X. Li, S. Tang, J.-Z. Zhao, J.-S. Han, K. Zhao, Z. Wang, and B. Xiao, "Communicating Is Crowdsourcing:Wi-Fi Indoor Localization with CSI-Based Speed Estimation," *JCST*, 2014.

[40] C. Wu, F. Zhang, Y. Hu, and K. J. R. Liu, "GaitWay: Monitoring and Recognizing Gait Speed Through the Walls," *IEEE TMC*, 2021.

[41] K. Niu, X. Wang, F. Zhang, R. Zheng, Z. Yao, and D. Zhang, "Rethinking Doppler Effect for Accurate Velocity Estimation With Commodity WiFi Devices," *IEEE JSAC*, 2022.

[42] M. Kotaru, K. Joshi, D. Bharadia, and S. Katti, "SpotFi: Decimeter Level Localization Using WiFi," in *Proceedings of ACM SIGCOMM*, 2015.

[43] "Free5GC: An Open-Source Project for 5th Generation Mobile Core Networks," https://free5gc.org/, 2023/10/20.

[44] Z. Wei, Y. Wang, L. Ma, S. Yang, Z. Feng, C. Pan, Q. Zhang, Y. Wang, H. Wu, and P. Zhang, "5G PRS-based Sensing: A Sensing Reference Signal Approach for Joint Sensing and Communication System," *IEEE TVT*, 2022.

[45] A. A. Abdallah, J. Khalife, and Z. M. Kassas, "Exploiting On-Demand 5G Downlink Signals for Opportunistic Navigation," *IEEE Signal Processing Letters*, 2023.

[46] C. R. Karanam, B. Korany, and Y. Mostofi, "Tracking from One Side: Multi-Person Passive Tracking with WiFi Magnitude Measurements," in *Proceedings of ACM/IEEE IPSN*, 2019.

[47] R. H. Venkatnarayan, M. Shahzad, S. Yun, C. Vlachou, and K.-H. Kim, "Leveraging Polarization of WiFi Signals to Simultaneously Track Multiple People," *Proceedings of ACM IMWUT*, 2020.

[48] L. Xu, X. Zheng, X. Li, Y. Zhang, L. Liu, and H. Ma, "WiCAM: Imperceptible Adversarial Attack on Deep Learning based WiFi Sensing," in *Proceedings of IEEE SECON*, 2022.

[49] W. Wang, L. Mottola, Y. He, J. Li, Y. Sun, S. Li, H. Jing, and Y. Wang, "MicNest: Long-Range Instant Acoustic Localization of Drones in Precise Landing," in *Proceedings of ACM SenSys*, 2022.

[50] W. Wang, J. Li, Y. He, and Y. Liu, "Symphony: Localizing Multiple Acoustic Sources with a Single Microphone Array," in *Proceedings of ACM SenSys*, 2020.

[51] W. Wang, Y. He, M. Jin, Y. Sun, and X. Guo, "Meta-Speaker: Acoustic Source Projection by Exploiting Air Nonlinearity," in *Proceedings of ACM MobiCom*, 2023.

[52] Y. Sun, W. Wang, L. Mottola, R. Wang, and Y. He, "AIM: Acoustic Inertial Measurement for Indoor Drone Localization and Tracking," in *Proceedings of ACM SenSys*, 2022.

[53] J. Zhang, R. Xi, Y. He, Y. Sun, X. Guo, W. Wang, X. Na, Y. Liu, Z. Shi, and T. Gu, "A Survey of mmWave-Based Human Sensing: Technology, Platforms and Applications," *IEEE Commun. Surv*, 2023.